

**SELECTED ACCELERATIONS AND ORBITAL
ELEMENTS OF THE GOCE SATELLITE
IN THE TIME DOMAIN**

Andrzej Bobojć

Institute of Geodesy
University of Warmia and Mazury in Olsztyn

Key words: GOCE satellite orbit, satellite accelerations, orbital elements, geopotential.

A b s t r a c t

The work contains the results of the GOCE satellite orbit simulation. The GOCE satellite orbit was presented in the aspect of the temporary changes in selected accelerations and in selected keplerian elements. The satellite accelerations due to: the geopotential, the Earth tides and the ocean tides (the radial component for both), the gravitation of the Moon and the gravitation of the Sun, were presented in function of time. The showed changes in orbital elements include the semi-major axis, eccentricity, inclination, argument of perigee and right ascension of ascending node. For the orbit determination the Cowell numerical integration method of the eighth order was used. The geopotential was described by means of the EGM96 model. The mentioned temporary changes in the selected accelerations and orbital elements were described. Most of them contain the characteristic periodic components, which are close to the satellite orbital period, the Earth's rotation period and the Moon's synodic period.

**WYBRANE PRZYŚPIESZENIA I ELEMENTY ORBITALNE SATELITY GOCE
W DZIEDZINIE CZASU**

Andrzej Bobojć

Instytut Geodezji
Uniwersytet Warmińsko-Mazurski w Olsztynie

Słowa kluczowe: orbita satelity GOCE, przyspieszenia satelity, elementy orbitalne, geopotencjał.

A b s t r a c t

Praca zawiera wyniki symulacji orbity satelity GOCE. Orbitę satelity GOCE przedstawiono w aspekcie zmian czasowych wybranych przyspieszeń i elementów keplerowskich. Przyspieszenia satelity spowodowane przez: geopotencjał, pływy skorupy, pływy oceaniczne (składowa radialna dla

obu), grawitację Słońca i grawitację Księżyca, przedstawiono w funkcji czasu. Pokazane zmiany w elementach orbity obejmują półoś wielką, mimośród, nachylenie, argument perygeum i rektascensję węzła wstępującego. Do wyznaczenia orbity użyto całkowania numerycznego metodą Cowella ósmego rzędu. Geopotencjał opisano modelem EGM96. Opisano wspomniane zmiany czasowe wybranych przyspieszeń i elementów orbity. Większość z nich zawiera charakterystyczne składowe okresowe, które są zbliżone do okresu orbitalnego satelity, okresu rotacji Ziemi oraz okresu synodycznego Księżyca.

Introduction

One of the ESA's missions is the Gravity Field and Steady – State Ocean Circulation Explorer Mission (GOCE). The GOCE mission has been started on 17 March 2009. The main goal of this mission is to determine the geopotential model up to 200 degree and order of the spherical harmonic coefficients. The mentioned model will allow to obtain the gravity acceleration with an accuracy of 1 mGal and to estimate of the geoid with an accuracy of 1 cm. Such accuracies will be realized at spatial scales down to 100 km (*Gravity Field...* 1999, DRINKWATER et al. 2003, MEGIE, READINGS 2000).

A gradiometric satellite is a key component of the GOCE mission. This satellite is placed into almost circular and sun-synchronous orbit with an average altitude of about 250 km (*Gravity Field...* 1999). The non-gravitational forces acting on the satellite are compensated by a drag-free control system (DRINKWATER et al. 2003). The GOCE satellite is planned to provide two types of measurements: the gravity gradients (Satellite Gravity Gradiometry data – SGG data) and the high-low Satellite to Satellite tracking data (SST data). They will be obtained by two on-board devices: an electrostatic gravity gradiometer and a GPS/GLONASS receiver, respectively (JOHANESSEN et al. 2003). Both the SGG data and the SST data will be subject of a joint inversion to estimate the Earth's gravity field model (DITMAR, KLEES 2002, DITMAR et al. 2003).

The knowledge of the satellite orbit is one of the key factors in the estimation of Earth's gravity field. GPS measurements (SST data) are the basic data for the GOCE satellite orbit estimation. Advanced algorithms were prepared to determine the aforementioned orbit in the form of a reduced-dynamic and a kinematic orbit solution (BOCK et al. 2006, VISSER et al. 2006).

Basically, the SGG data (i.e. gravity gradients) will be used to obtain the Earth's gravity field model. However, these observations also carry the information about the position and velocity of a satellite. Thus they can be used in the process of satellite orbit improvement. This process requires the computation of approximated gravity gradients along a approximated orbit. The description of planned GOCE satellite orbit using the temporary changes in the selected accelerations and in keplerian elements, can be helpful in the computation of aforementioned approximated orbit.

Simulations

To obtain the GOCE satellite orbit, the Cowell numerical integration method of the eighth order was used. The computed orbit was expressed with respect to the J2000.0 reference frame (LAING 1991, ANDERSON et al. 2002). This frame can be described in the following way: the origin at the Earth's mass centre, the X-axis is directed towards the mean vernal equinox of the standard epoch J2000.0 (at noon on January 1, 2000), the Z-axis points out from the Earth's mass centre along the Earth's mean rotational axis of the standard epoch J2000.0, the Y-axis completes the frame to the right-handed frame. The following initial elements of the GOCE orbit were taken into the computation: the epoch: 54313.0 MJD, semi-major axis: 6634.7711 km, eccentricity: 0.001, inclination: 96.5 deg., argument of perigee: 0.00 deg., right ascension of ascending node: 45.00 deg., mean anomaly: 0.00 deg., the orbital period $T = 89.64$ min. (*Gravity Field...* 1999). The computations were performed using the TOP package (DROŻYNER 1995). The TOP package determines a satellite orbit in the Earth's gravity field taking into account selected perturbing forces. Several models were used to the orbit computation. The EGM96 model (LEMOINE et al. 1998) was taken for the geopotential. The Earth and ocean tides were modelled by the MERIT Standards (MELBOURNE et al. 1983). Both, the IAU1976 Theory of Precession and the IAU1980 Theory of Nutation (the Wahr nutation) were included to the computation. Additionally, the following data were taken into the computation: the Sun, Moon and planet ephemerides DE200/LE200 (epoch J2000.0). The pole coordinates were equal to zero.

It was assumed that the GOCE satellite motion is determined by the geopotential and by the following forces: the gravitation of the Moon, the gravitation of the Sun, the gravitation of the planets, the Earth tides and the ocean tides. Additionally, the relativity effects was taken into account in the satellite motion model. The relativity effects generate the corresponding satellite acceleration. Taking into account the aforementioned assumptions, a 30-day arc of the GOCE orbit with an integration step 60 s was obtained. The chosen satellite accelerations due to the mentioned above forces and the chosen keplerian elements, were computed along this orbit. The obtained temporary changes of the selected accelerations and keplerian elements were expressed with respect to the J2000.0 reference frame.

Description of the obtained temporary changes

The presented below graphs were prepared for the 30-day arc of the GOCE orbit. The initial epoch (denoted as 0) and the last given epoch (number 21600) correspond to 54313.0 MJD and 54343.0 MJD, respectively. A sampling

interval is 2 minutes. For most presented below figures, the main graph and additional small graphs were prepared. These small graphs zoom in the main graph in the chosen epoch ranges of the 30-day orbital arc. The width of these ranges is 400 minutes with the exception of Figure 9b, where the mentioned width is equal to 200 minutes.

The term “amplitude” used in this work, refers to the difference between a given maximum and a neighbouring minimum (so called peak-to-peak amplitude).

Changes in selected accelerations

The temporary changes of the satellite acceleration due to the geopotential are presented in Figure 1. The continuous oscillations of the mentioned acceleration result from this figure. The acceleration oscillates around the value of $\sim 9.062 \text{ m s}^{-2}$ (Fig. 1a). These oscillations have the periodic behavior with the increasing amplitude. At the start of the orbital arc, this amplitude is equal to about 0.04 m s^{-2} . Next, it decreases to approx. 0.03 m s^{-2} (at \sim one-fifth of the orbital arc) and increases to about 0.09 m s^{-2} at the end of the orbital arc. An occurrence of the oscillation of the geopotential-derived acceleration is in relation with the non-zero value of eccentricity (for the initial epoch 0.001). As the additional research showed, the increasing trend of the eccentricity appears together with the mentioned increase of the oscillating amplitude of the acceleration. Two periods of the acceleration changes can be seen in Figure 1. The first period visible in four small graphs of Figure 1 is equal to about 90 minutes and coincides with the satellite orbital period. The second period is equal to about 1 day and is close to the Earth’s rotation period. This period concerns the changes of the maximum values of acceleration and is visible in Figure 1a. The occurrence of the aforementioned period is in relation with the Earth’s rotation with respect to the used J2000.0 frame.

In the first three small graphs (Fig. 1b-1d), the characteristic small peaks between the main peaks of the oscillating acceleration, are shown. The mentioned peaks appear in the middle of the satellite orbital period. Taking into account Figure 1b, the explanation of such acceleration changes can be performed. The satellite experiences the maximum acceleration at the perigee, being simultaneously at the equatorial plane, near the equatorial bulge (the acceleration at the epoch 0 in Fig. 1b). Next, the acceleration decreases when the satellite moves around the Earth. When the satellite reaches the maximum altitude above the equatorial plane, after the quarter of the orbital period, the acceleration decreases to the minimum value. From this point, the experienced acceleration increases when the satellite returns to the equatorial plane. After half the orbital period, the satellite is again at the equatorial plane, near the

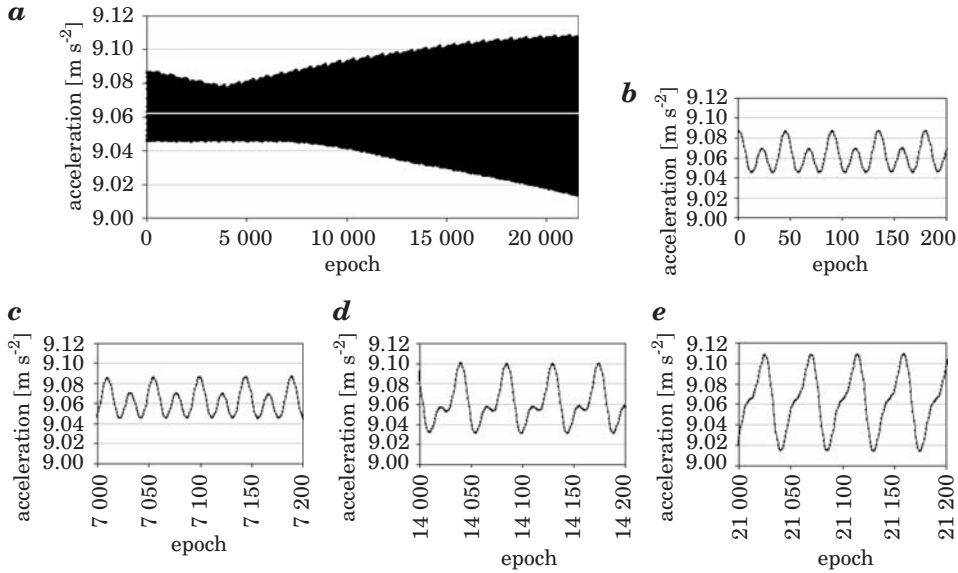


Fig. 1. The acceleration due to the geopotential along the 30-day orbit with the 2 minute sample interval. The epoch 0 and the last showed epoch correspond to 54313.0 MJD and 54343.0 MJD, respectively. The group of the small graphs presents the parts of the main graph in the chosen epoch ranges

equatorial bulge. At this point, the acceleration reaches the maximum value (the mentioned small peak, Fig. 1*b*). However, this maximum is smaller than the former one due to the apogee of the orbit. Then, the acceleration again decreases during the satellite travel under the equatorial plane. It reaches the minimum when the distance between the satellite and the equatorial plane has the maximum value. This point of the orbit corresponds to three-quarters the orbital period. Next, the acceleration increases – the satellite approaches again the equatorial plane. After the orbital period, the satellite is at the perigee and the acceleration has again the maximum value. The similar changes of acceleration (as in Fig. 1*b*) are given in Figure 1*c*. In two remaining Figures 1*d* and 1*e*, the acceleration changes differ from those showed in Figures 1*b* and 1*c*. The oscillation amplitude is greater and the small peaks of the acceleration are less clear in Figures 1*d* and 1*e*. Especially in Figure 1*e*, where only the remains of these peaks can be noticed. Such acceleration changes indicate an evolution of the orbit in the inhomogeneous gravity field of the oblated Earth and under the influence of other perturbing forces. As mentioned above, the increasing oscillation amplitude of acceleration is connected with the increasing eccentricity trend, whereas the change of the small peaks of acceleration in Figures 1*b*–1*e*, is in relation with the change of the argument of perigee.

The radial component of acceleration generated by the Earth tides is given in Figure 2. This component oscillates with a period of about 45 minutes (Fig. 2*b–e*), which is close to half the orbital period of the satellite. Such period can be related to the Earth’s oblateness. The satellite passes through the equatorial plane every approx. 45 minutes (half the orbital period). When the satellite is near this plane, the radial acceleration induced by the Earth tides reaches the minimum value. Additionally, the main graph (Fig. 2*a*) presents the maximum and minimum acceleration changes with the period of about 0.5 day and the oscillation amplitude changes with the period of about 29–30 days (close to the Moon’s synodic period). This reflects the impact of an Earth-Moon-Sun configuration on the Earth tides. The values of presented radial acceleration change in the range from $-3.67 \cdot 10^{-7} \text{ m s}^{-2}$ (towards the Earth’s mass centre) to about $3.75 \cdot 10^{-7} \text{ m s}^{-2}$ (towards the opposite direction with respect to the Earth’s mass centre direction). This means that in the satellite motion, an “undulate” component appears. A time interval of sign change of the acceleration is about 22–23 minutes (Fig. 2*d*). After such interval an action direction of this radial component changes.

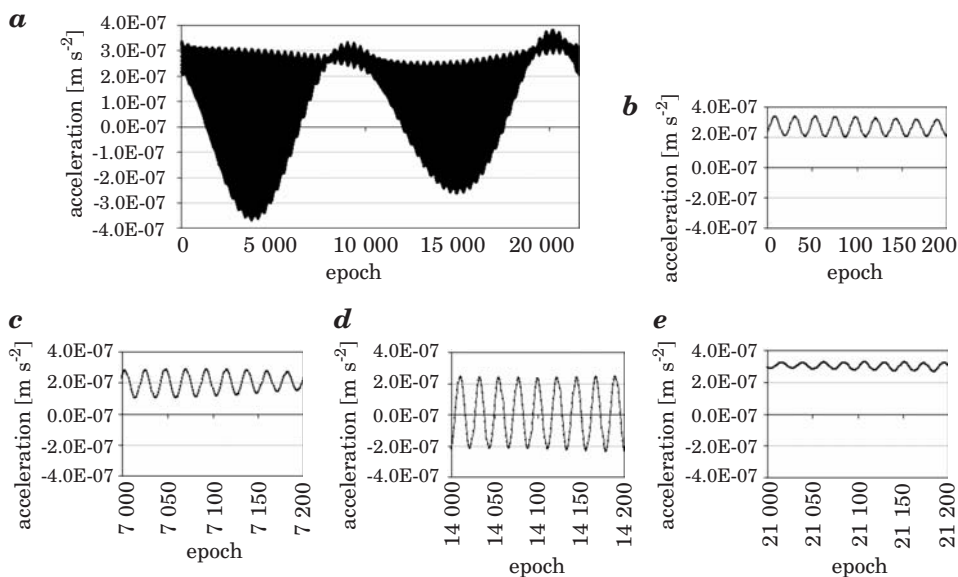


Fig. 2. The radial component of acceleration generated by the Earth’s tides along the 30-day orbit with the 2 minute sample interval. The epoch 0 and the last showed epoch correspond to 54313.0 MJD and 54343.0 MJD, respectively. The group of the small graphs presents the parts of the main graph in the chosen epoch ranges

The radial component of the satellite acceleration generated by the ocean tides is given in Figure 3. It is clear visible that it oscillates around zero (Figures 3a–3e). The values place in the range between $-3.56 \cdot 10^{-7} \text{ m s}^{-2}$ to about $3.40 \cdot 10^{-7} \text{ m s}^{-2}$. Figure 3a shows a faint period of the change of oscillation amplitude. It equals approx. 14–15 days (almost half the Moon’s synodic period). However, this period, taking into account the 30-day limitation of the simulated orbital arc, can be a harmonic of the Moon’s synodic period (29.5 days) also occurring in the presenting changes. The oscillations given in Figures 3b–3e seem to be irregular. This oscillation irregularity maybe caused by the “water” nature of ocean tides. A minimum time interval of sign change for the described acceleration is about 4 minutes (Fig. 3e), i.e. the action direction of acceleration changes after such interval.

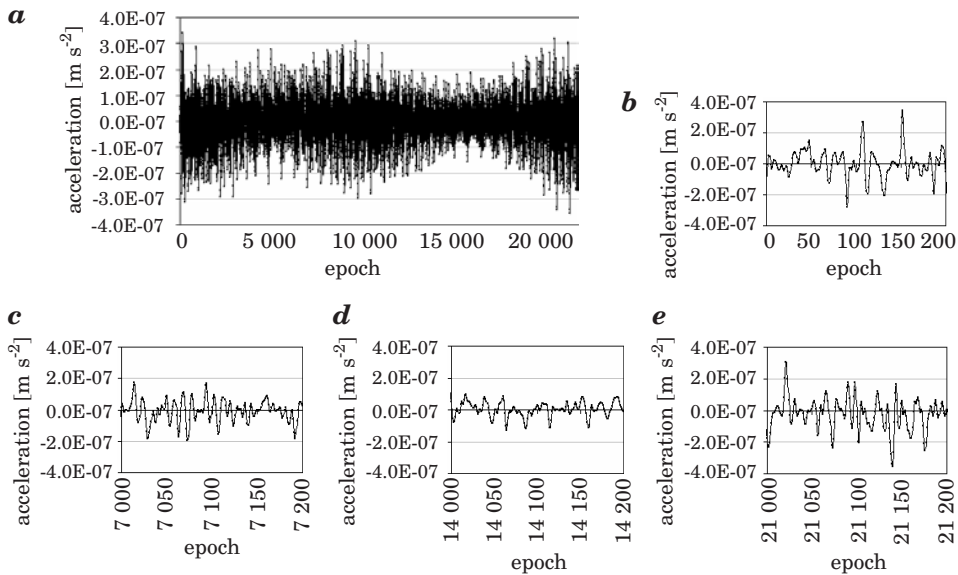


Fig. 3. The radial component of acceleration due to the ocean tides along the 30-day orbit with the 2 minute sample interval. The epoch 0 and the last showed epoch correspond to 54313.0 MJD and 54343.0 MJD, respectively. The small graphs are the parts of the main graph in the chosen epoch ranges

The satellite acceleration due to the gravitation of the Moon is presented in Figure 4. The showed oscillations of the acceleration are very regular here. The visible changes of the oscillation amplitude are in relation with the Moon motion with respect to the satellite orbital plane. Three periods of the oscillating acceleration can be seen in Figure 4. The first period of the changes of the oscillation amplitude is equal to approx. 29–30 days (Fig. 4a). The second

period of acceleration changes has the value of about 45 minutes (near half the orbital period, Fig. 4b and 4e). Finally, the period visible in Figures 4c and 4d is equal to about 90 minutes. Similarly as for the acceleration generated by the geopotential, the smaller “peaks” occur between the successive larger “peaks” of acceleration value. In this case the difference between the large “peaks” and the small ones is noticeable smaller (Fig. 4c and 4d). The considered acceleration varies from $4.90 \cdot 10^{-7} \text{ m s}^{-2}$ to about $1.31 \cdot 10^{-6} \text{ m s}^{-2}$ (Fig. 4a).

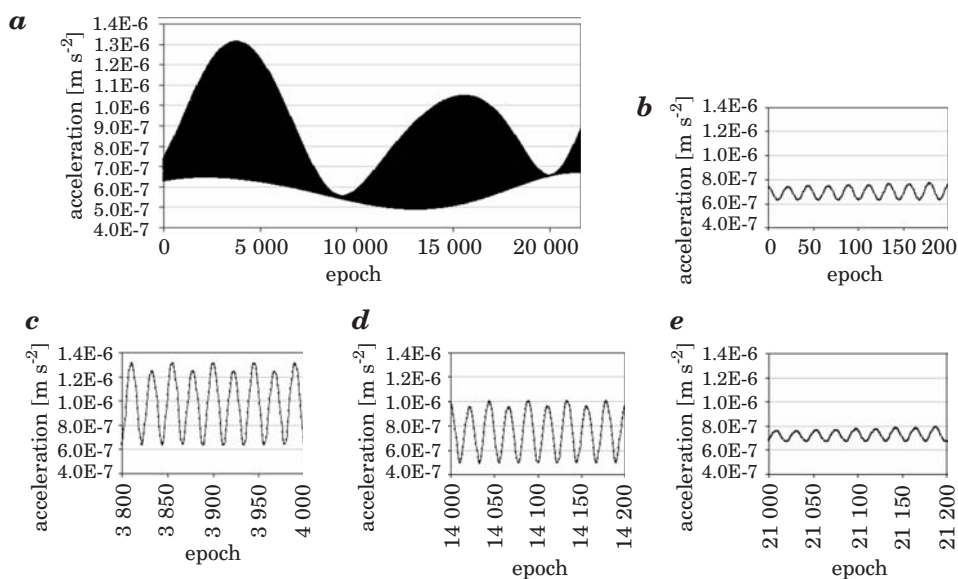


Fig. 4. The acceleration generated by the gravitation of the Moon along the 30-day orbit with the 2 minute sample interval. The epoch 0 and the last showed epoch correspond to 54313.0 MJD and 54343.0 MJD, respectively. The group of the small graphs presents the parts of the main graph in the chosen epoch ranges

The changes of the satellite acceleration under the influence of the gravitation of the Sun are presented in Figure 5. A characteristic feature of these changes is the decreasing oscillation amplitude. This amplitude varies from approx. $1.7 \cdot 10^{-8} \text{ m s}^{-2}$ (at the start of orbital arc) to about $5.0 \cdot 10^{-9} \text{ m s}^{-2}$ (at the end of orbital arc). Thus, an angle between the satellite orbital plane and the Earth-Sun direction increases in the whole 30-day interval of the orbit. The showed acceleration is placed between $\sim 2.51 \cdot 10^{-7} \text{ m s}^{-2}$ and $\sim 2.68 \cdot 10^{-7} \text{ m s}^{-2}$. Similarly as for the acceleration generated by the gravitation of the Moon, two typical periods with the length of ~ 45 minutes and of ~ 90 minutes can be

noticed in Figures 5b–5e. Unlike the acceleration generated by the Moon, the smaller minimum appears here in the middle of orbital period between successive larger minimums of the acceleration (Fig. 5d, 5e).

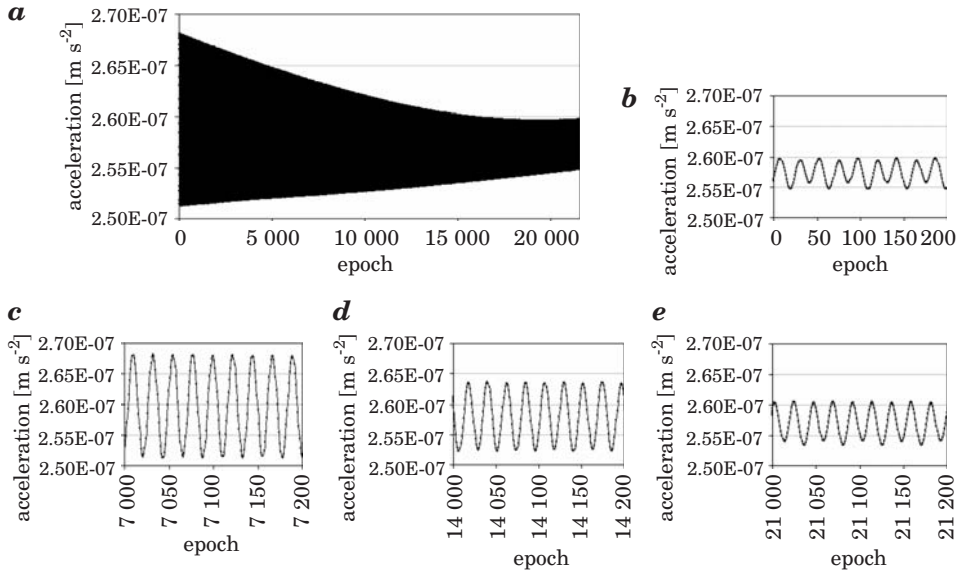


Fig. 5. The acceleration generated by the gravitation of the Sun along the 30-day orbit with the 2 minute sample interval. The first showed epoch and the last showed one correspond to 54313.0 MJD and 54343.0 MJD, respectively. The small graphs present the parts of the main graph in the chosen epoch ranges

Changes in selected orbital elements

Figure 6 shows the semi-major axis for the considered 30-day orbital arc. This orbital element oscillates very regularly with a period of about 45 minutes around the value of about 6624.53 km (Fig. 7a and 7b). The amplitude of these oscillations is almost constant and equals to approx. 19.54 km. The presence of the 45-minute period of the semi-major axis changes is caused mainly by the satellite orbit perturbation due to the Earth's oblateness. In his orbital motion, the satellite is over the equatorial plane during half the orbital period (just about 45 minutes) and under this plane during half the orbital period, too. The symmetric mass distribution with respect to the equatorial plane (in some approximation) decides about the occurrence of just 45-minute period.

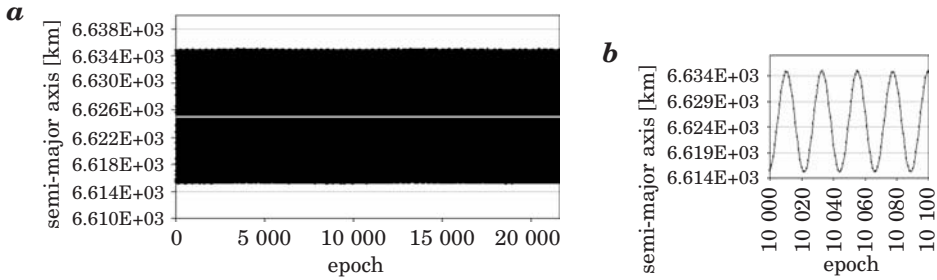


Fig. 6. The semi-major axis of the keplerian osculating orbit along the 30-day orbital arc with the 2 minute sample interval. The epoch 0 – 54313.0 MJD, the last showed epoch – 4343.0 MJD. The small graph gives the part of the main graph in the chosen epoch range. The white line denotes the trend line

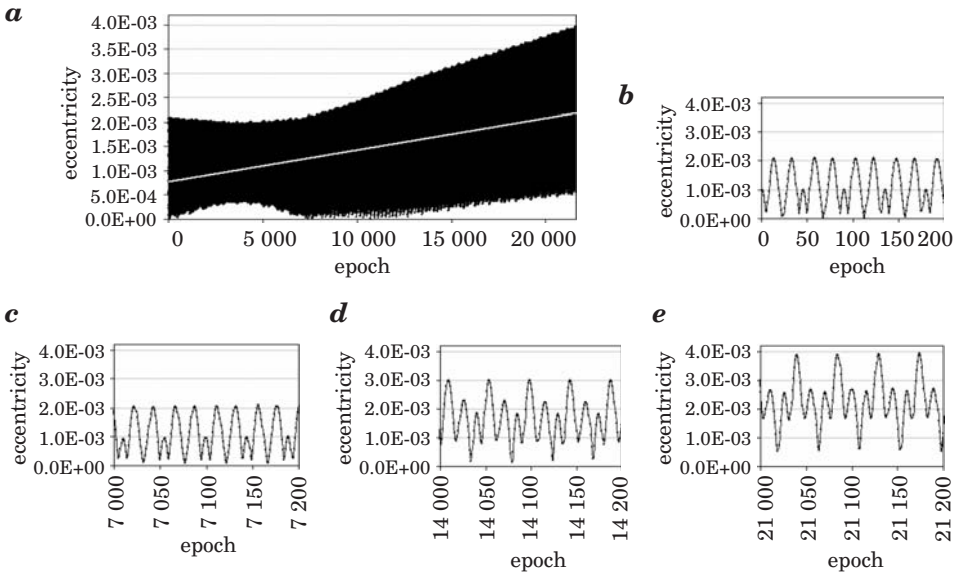


Fig. 7. The eccentricity of the keplerian osculating orbit along the 30 – day orbit arc with the 2 minute sample interval. The epoch 0 and the last showed epoch correspond to 54313.0 MJD and 54343.0 MJD, respectively. The small graphs give the parts of the main graph in the chosen epoch ranges. The white line is the trend line

In the case of eccentricity, the changes are fairly complex (Fig. 7). The oscillation amplitude decreases from about $2.0 \cdot 10^{-3}$ to near $1.6 \cdot 10^{-3}$ at one-fifth of the orbital arc and then it increases to approx. $3.4 \cdot 10^{-3}$ at the end of orbital arc (Fig. 7a). The increasing trend occurs in the visible changes. The given values of eccentricity are placed between about $1.81 \cdot 10^{-5}$ to near $3.97 \cdot 10^{-3}$. As it results from Figure 7a, the minimum and maximum values of eccentricity changes with about the 1-day period. The period equal to

~ 90 minutes is visible in Figures 7b–7e. The changing profile of oscillation is given in these figures, too. In this profile, a smaller maximum lies (in the middle of the orbital period) between two the same greater maximums (Fig. 7b and 7c). Next, the dominant maximum arises from the previous smaller maximum, lying between two smaller maxima (Fig. 7d and 7e).

The changes of the inclination with its increasing trend are showed in Figure 8a. Two periods of the oscillation are visible here. The length of the first period is equal to about 14 days (near half the Moon’s synodic period), whereas the second one has the length of near 0.5 day and is connected with the changes of maximum and minimum inclination values. The oscillation amplitude is equal to ~ 0.01 degree and it remains almost constant for the whole orbital arc. From Figure 8, the range of inclination values between 96.499 degrees to 96.526 degrees results. Figures 8b–8e present the basic oscillations of inclination with the period close to 45 minutes (near half the satellite orbital period). The visible periods and the increasing trend of inclination are caused mainly by the inhomogeneous Earth’s gravity field. Additional research showed that the occurrence of the 14 day period is generated also by the gravitation of the Moon and by the tides (mainly by the Earth tides), whereas the increasing trend of inclination is caused, in a less degree, by the gravitation of the Sun, the gravitation of the Moon and the Earth tides.

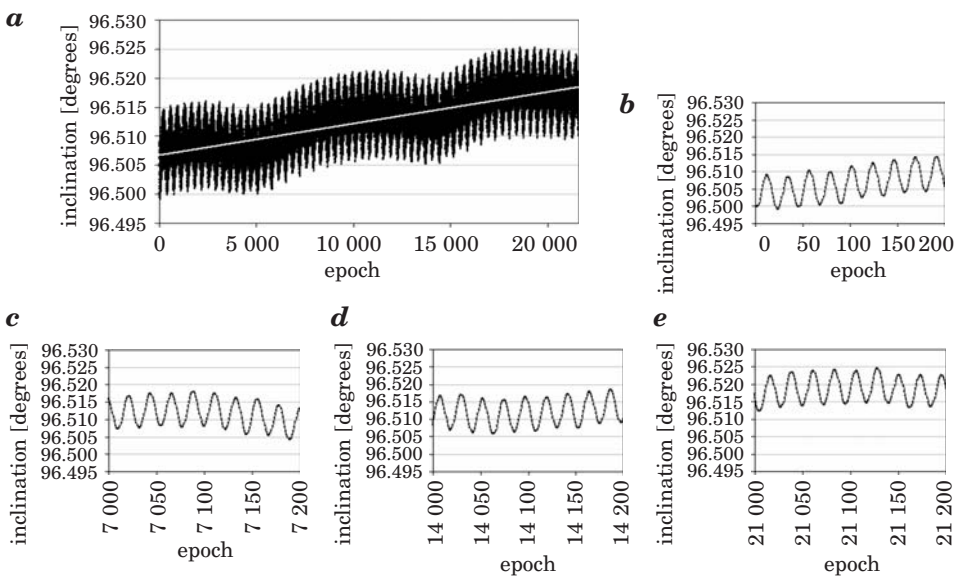


Fig. 8. The inclination of the keplerian osculating orbit along the 30 – day orbit arc with the 2 minute sample interval. The epoch 0 and the last showed epoch correspond to 54313.0 MJD and 54343.0 MJD, respectively. The small graphs contain the parts of the main graph in the chosen epoch ranges. The white line is the trend line

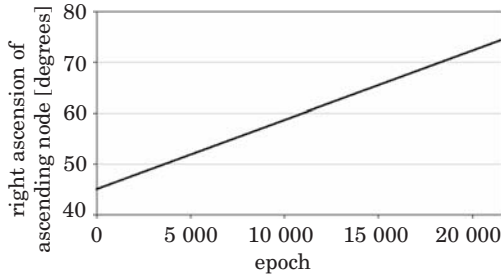


Fig. 9. The right ascension of ascending node of the keplerian osculating orbit along the 30 – day orbit arc with the 2 minutes sample interval. The epoch 0 and the last showed epoch correspond to 54313.0 MJD and 54343.0 MJD, respectively

The characteristic changes of the right ascension of ascending node are given in Figure 9. This orbital element linearly increases from 45 degrees to about 74.4 degrees under the influence of the inhomogeneous Earth’s gravity field.

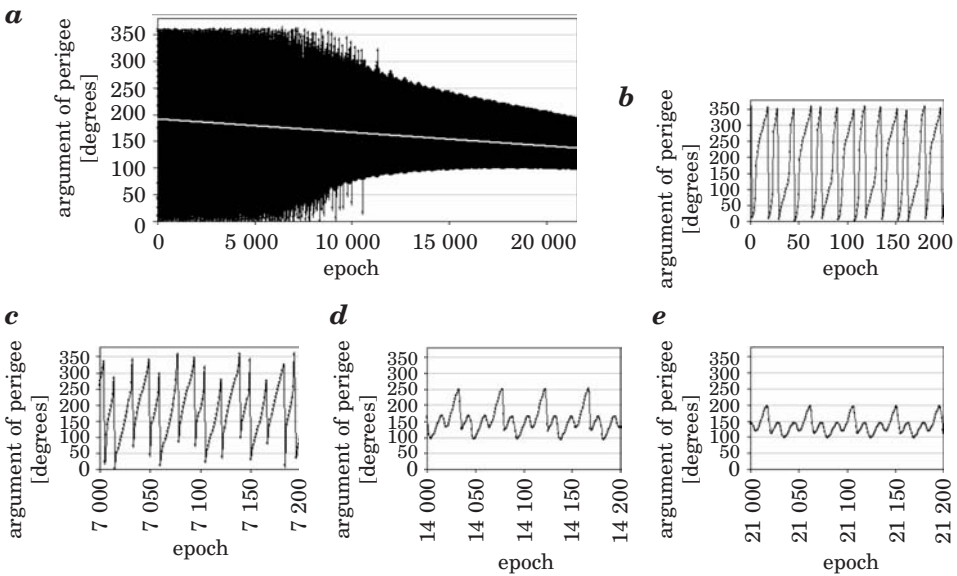


Fig. 10. The argument of perigee of the keplerian osculating orbit along the 30 – day orbit arc with the 2 minutes sample interval. The epoch 0 and the last showed epoch correspond to 54313.0 MJD and 54343.0 MJD, respectively. The small graphs present the parts of the main graph in the chosen epoch ranges. The white line is the trend line

Figure 10 presents the changes of the argument of perigee. These changes are deformed by a numerical noise for about half the orbital arc (Figures 10a–10c). The aforementioned numerical noise can be connected with the small value of eccentricity (initially – 0.001). After half the orbital arc the

argument of perigee oscillates more regularly with the period of near 90 minutes (Figures 10*d* and 10*e*). Between the successive higher maxima the minimum occurs in the middle of the satellite orbital period. For both part this minimum, two smaller maxima are visible (Fig. 10*d* and 10*e*). The oscillation amplitude decreases to about 100 degrees simultaneously with the decreasing trend of value (Fig. 10*a*).

Summary

The changes of the selected accelerations and orbital elements were determined for the GOCE satellite. In most cases these changes can be characterized by the oscillations with the exception of the right ascension of ascending node, which changes linearly. In two cases, the characteristic profile of the changes of the oscillation amplitude occurred. Namely, the decrease of amplitude from the start of orbital arc to about one-fifth of its length and then the increase to the end of orbital arc. In this way, the oscillation amplitude of the geopotential derived acceleration and of the eccentricity varies. The following approximated periods were noticed in the presented temporary changes:

- 45-minute period (close to half the orbital period) – the changes of: the radial component of acceleration due to the Earth tides, the accelerations due to the gravitation of the Moon and of the Sun, the semi-major axis and the inclination,
- 90-minute period (close to the orbital period) – the changes of: the geopotential derived acceleration, the acceleration due to the gravitation of the Moon and of the Sun, the eccentricity and the argument of perigee,
- 0.5-day period (half the Earth's rotation period) – the changes of: the radial component of acceleration due to the Earth tides (for the minimum and maximum values), the inclination (for the minimum and maximum values, too),
- 1-day period (the Earth's rotation period) – the changes of: the geopotential derived acceleration (for the maximum values), the eccentricity (for the minimum and maximum values),
- 14–15 day period (close to half the Moon's synodic period) – the changes of: the radial component of acceleration due to the ocean tides (for the oscillation amplitude), the inclination,
- 29–30 day period (close to the Moon's synodic period) – the changes of: the acceleration due to the gravitation of the Moon (for the oscillation amplitude), the radial components of acceleration due to the Earth tides and the ocean tides (for the oscillation amplitude; in this case the period of 29–30 days results indirectly from Figures 2, 3, 4.

The basic periods of the showed changes are equal to about 45 and 90 minutes. The longer periods concern usually the changes of the minimum and maximum values or the oscillation amplitude.

The changes of presented orbital elements reflect the combined perturbations mainly coming from the Earth's gravity field. The perturbations in the GOCE orbital elements under the influence of separate forces can be the subject of the another work.

Accepted for print 11.08.2009

References

- ANDERSON J.D., LAING P.A., LAU E. L., et al. 2002. *Study of the anomalous acceleration of Pioneer 10 and 11*. Phys. Rev. D65 082004.
- BOCK H., JÄGGI A., SVEHLA D. 2007. *Precise Orbit Determination for the GOCE Satellite Using GPS*. Adv. Space Res., 39: 1638–1647.
- DITMAR P., KLEES R. 2002. *A Method to Compute the Earth's Gravity Field from SGG/SST data to be Acquired by the GOCE Satellite*. Delft University Press.
- DRINKWATER M.R., FLOBERGHAGEN R., HAAGMANS R. et al. 2003. *GOCE: ESA's First Earth Explorer Core Mission*. Space Science Reviews, 00: 1–14.
- DROŻYNER A. 1995. *Determination of Orbits with Toruń Orbit Processor System*. Adv. Space Res., 16(2). *Gravity Mission – GOCE Brochure* (revised). 2006. ESA's.
- Gravity Field and Steady-State Ocean Circulation Mission, ESA SP-1233(1)*. 1999. ESA. Report for mission selection of the four candidate Earth Explorer missions.
- JOHANNESSEN J.A., BALMINO G., LE PROVOST C. et al. 2003. *The European Gravity Field and Steady-State Ocean Circulation Explorer Satellite Mission Its Impact on Geophysics*. Surveys in Geophysics, 24(4): 339–386.
- LAING P.A. 1991. *Implementation of J2000.0 reference frame in CHASMP*. The Aerospace Corporation's Internal Memorandum, 91(6703).
- LEMOINE F., KENYON S., FACTOR J. 1998. *The Development of the Joint NASA GSFC and the National Imagery and Mapping Agency (NIMA) Geopotential Model EGM96*. Report No.206861.
- MELBOURNE W. 1983. *Project MERIT Standards*. Circ. 167, U.S. Naval Observatory, Washington, D.C.
- MÉGIE G., READINGS C. J. 2000. *The Earth Explorer Missions – Current Status*. Earth Observation Quarterly No. 66.